HAYATI
Journal of Biosciences

Vol. 33 No. 1, January 2026 167-180
DOI:10.4308/hjb.33.1.167-180
ISSN: 1978-3019
EISSN: 2086-4094

Research Article

Anticancer Activities and Metabolite Profiling of UHPLC-HRMS Method from *Chrysanthemum x morifolium* (Ramat.) Hemsl Leaves

Imas Maesaroh[1,2], Melisa Intan Barliana[3,4], Rizky Abdulah[4,5], Muhaimin Muhaimin[3,6*]

[1]*Doctoral Program of Pharmacy, Faculty of Pharmacy, Universitas Padjadjaran, Sumedang 45363, Indonesia*
[2]*Faculty of Pharmacy, Health and Science, Universitas Muhammadiyah Kuningan, Kuningan 45552, Indonesia*
[3]*Department of Biological Pharmacy, Faculty of Pharmacy, Universitas Padjadjaran, Jatinangor 45363, Indonesia*
[4]*Center of Excellence in Pharmaceutical Care Innovation, Universitas Padjadjaran, Jatinangor 45363, Indonesia*
[5]*Department of Pharmacology and Clinical Pharmacy, Faculty of Pharmacy, Universitas Padjadjaran, Jatinangor 45363, Indonesia*
[6]*Center for Herbal Studies, Universitas Padjadjaran, Jatinangor 45363, Indonesia*

ARTICLE INFO

Article history:
Received January 17, 2025
Received in revised form September 2, 2025
Accepted October 10, 2025
Available Online October 16, 2025

KEYWORDS:
Chrysanthemum morifolium,
cytotoxic activity,
MCF-7,
metabolite profiling

ABSTRACT

The *Chrysanthemum morifolium* Ramat, traditionally used for cancer treatment, including breast cancer, possesses anticancer properties. The aim of this study is metabolite profiling using ultra-high-performance liquid chromatography in conjunction with the high-resolution mass spectrometry (UHPLC-HRMS) technique and its correlation with the cytotoxic activity of the extract and ethyl acetate fraction of *Chrysanthemum x morifolium* (Ramat.) Hemsl leaves on cancer cells. The ethyl acetate fraction from the hydrolyzed ethanol extract of (*Chrysanthemum x morifolium* (Ramat.) Hemsl) leaves has anticancer activity against the MCF-7 breast cancer cells. Metabolite profiling was used to understand the presence of metabolites that have anticancer activity. UHPLC-HRMS was used to profile their metabolites. Compound Discoverer 3.3 software finished data processing and metabolite annotation. Anticancer activity was performed using the 2-[2-methoxy-4-nitrophenyl]-3[4-nitrophenyl]-5[2,4-disulfophenyl]-2H-tetrazolium (WST-8) assay. As many as 57 secondary metabolites were identified by UHPLC-HRMS analysis. Secondary metabolites that have the potential as anti-breast cancer are glycitein, diosmetin, kaempferol, esculetin, scopoletin, dihydroartemisinin, and Chrysin, with successive percentages of 31.39%, 19.91%, 5.61%, 2.63%, 0.82%, 0.14%, and 0.05%. Ethyl acetate fraction showed stronger cytotoxic activity than ethanol extract against MCF-7 cells with IC_{50} values of 66.31 ppm at 24 hours incubation and 40.35 ppm at 48 hours. Further research can be conducted on the isolation of flavonoids from the ethyl acetate fraction, as well as the analysis of cell cycle apoptosis stimulation and gene expression mechanisms.

1. Introduction

Cancer is a non-communicable disease that affects people all around the world. According to the World Health Organization (WHO), cancer is one of the leading causes of mortality globally. The data from the World Health Organization's Global Burden of Cancer (GLOBOCAN) shows that there were 18.1 million cases and 9.6 million deaths from cancer as of 2018. It is anticipated that by 2030, there will be over 13.1 million cancer-related deaths (Bray *et al.* 2018). With 2,261,419 new cases or 11.7% of all cases worldwide, breast cancer has the highest death toll (684,996 cases, or 6.9% of all cases), with 58,256 instances, or 16.7% of all cases, occurring in Indonesia out of 348,809 total cases of cancer. In the meantime, about 22,692 cases resulted in deaths (Kemenkes RI 2019; Sung *et al.* 2021). By 2023, it is anticipated that 297,790 women in the US will be diagnosed with invasive breast cancer, whereas 55,720 women will be diagnosed with non-invasive breast cancer (in situ) (Siegel *et al.* 2023).

As a prominent herbal medicine used in China, South Korea, Thailand, and Japan, *Chrysanthemum*

*Corresponding Author
E-mail Address: muhaimin@unpad.ac.id

morifolium Ramat is a member of the Asteraceae family and is commonly consumed as a health drink. It has also been cultivated as an ornamental plant (Cai *et al.* 2021). Indonesia produced 394.502.028 *Chrysanthemum blooms* in 2022, the most of any other floriculture plant (BPS 2022). Many studies have shown that *Chrysanthemum morifolium* Ramat has anticancer properties. It has been widely used traditionally to treat cancer, including breast cancer (Hodaei *et al.* 2021a), lung cancer (Ma *et al.* 2021), leukemia (bin Muhamad Noor *et al.* 2021), colon cancer (Xie *et al.* 2009), and stomach cancer (Liu *et al.* 2018). Studies on *Chrysanthemum cinerariifolium* as an anti-breast cancer and oral squamous carcinoma (Lestari *et al.* 2019; Mutiah *et al.* 2020a, 2020b, 2021) and *Chrysanthemum boreal* as an anti-pulmonary, prostate, and colon cancer (Park *et al.* 2009) have shown the usage of leaves from the genus *Chrysanthemum* as having anticancer activity.

The most prevalent flavonoid components in *Chrysanthemum morifolium* flowers are luteolin and rutin (Hodaei *et al.* 2021b). Flavonoids are natural compounds of interest as potential candidates for developing anticancer drugs. They exhibit anticancer activity through various mechanisms of action, including inhibition of cancer cell growth, induction of apoptosis, and inhibition of angiogenesis. It has been shown that flavonoids interact with a wide range of genes and enzymes, including those involved in anti-proliferation, cell cycle suspension, apoptosis, angiogenesis, and multidrug resistance (Obakan-yerlikaya *et al.* 2017). Inhibiting the protein p53 tumor gene mutation is one way that the flavonoid compound helps prevent excessive cell proliferation and increased cell death in breast cancer (Dermawan *et al.* 2019). Flavonoid compounds (Chalcone and its derivatives) are thought to inhibit Estrogen Receptor α (REα), which acts as an anti-breast cancer agent (Muchtaridi *et al.* 2017). 17 β estradiol (E2) and Cisplatin can activate REα and cause platinum resistance. For malignancies resistant to platinum, REα could be a promising therapeutic target (Matsumura *et al.* 2017).To achieve this aim, we employed metabolite profiling to determine the presence of secondary metabolites, such as flavonoids, which have the potential to act as breast cancer inhibitors. The field of ophthalmology of secondary metabolites in natural goods or plants has advanced significantly in recent years. Compared to the Bioassay Guided Isolation technique, this technique has the advantage of a shorter active compound discovery stage using fewer samples. This technique can be done quickly using the UHPLC-HRMS instrument. Based on this description, the following is a study of metabolite profiling and its correlation with the cytotoxic activity of the extract and ethyl acetate fraction of (*Chrysanthemum x morifolium* (Ramat.) Hemsl) leaves on cancer cells.

2. Materials and Methods

2.1. Plant Material

(*Chrysanthemum x morifolium* (Ramat.) Hemsl.) leaves were collected from the Chrysene plantation in the hamlet of Canoe, Bandungan district, Semarang district, Central Java Province, during the full flowering stage in June 2023. The Plant determination was used in the Biosystematics and Molecular Laboratory, Department of Biology, Faculty of Mathematics and Natural Sciences, Padjadjaran University, to identify (*Chrysanthemum x morifolium* (Ramat.) Hemsl) Leaves. Samples were dried at room temperature.

2.2. Chemicals

Water (hypergrade for LC-MS), formic acid (hypergrade for LC-MS), methanol (hypergrade for LC-MS), ethanol 70% (Merck), $NaHCO_3$, Ethyl acetate (Merck), Chloroform p.a (SmartLab), methanol p.a (SmartLab), silica gel plate GF254 (Merck), aqua pro injection, formic acid 0.1%. For cytotoxic assay cell culture MCF-7 (ATCC HTB-22), DMSO (Dimethyl sulfoxide) (Sigma Aldrich), medium DMEMDubecco's's Modified Eagle Medium), PBS (Phosphate Buffer Saline) (Sigma Aldrich), Cisplatin (Merck), and WST-8 reagent (Dojindo).

2.3. Instrumentation

The use of instruments was needed to get the results of this research. The researcher used Analytics balance (Ohaus), Autoclave (Hirayama - Hiclave - HVE 50), Biology safety cabinet (Esco), centrifuge (Dlab), rotary evaporator (IKA), water bath (Memmert, Yihder BT-150D), micropipette (Eppendorf), hemocytometer (Marienfeld), inverted microscope (Zeiss), incubator CO2 (Thermo Scientific), 96- well plate, microplate reader (Tecan nano quant infinite M200pro), microtubule (Genfollower) and vortex mixer (Thermoline), Magnetic stirrer (MR-Hei), pHmeter (Hanna), LC (Thermo Scientific™ Vanquish™ UHPLC Binary Pump) and Orbitrap high-resolution mass spectrometry (Thermo Scientific™ Q Exactive™ Hybrid Quadrupole-Orbitrap™ High-Resolution Mass Spectrometer), column Thermo Scientific™ Accucore™ Phenyl-Hexyl 100 mm × 2.1 mm ID × 2.6 µm.

2.4. Procedure

2.4.1. Sample Extraction

Air-dried powdered leaves (250 g) were extracted with 70% ethanol (1:10 w/v) by maceration for 24 hours and remaceration (x3) at room temperature. The ethanol was evaporated in a vacuum (IKA)—a rotary evaporator operating at 50°C and 75 rotations per minute. A thick extract was obtained by heating the evaporation results over a water bath (Memmert, Yihder BT-150D) heated to 50°C to yield crude extracts as follows (92.53 g). The yield is the percentage of the raw materials that are used to produce a product.

2.4.2. Hydrolysis and Partitioning (*Chrysanthemum x morifolium* (Ramat.) Hemsl) Leaves Ethanol Extract

After adding 2N HCl (1:2) to 5 g of (*Chrysanthemum x morifolium* (Ramat.) Hemsl) leaves ethanol extract, it was hydrolyzed and homogenized for an hour at room temperature using a magnetic stirrer hot plate (MR-Hei). Next, add sodium bicarbonate ($NaHCO_3$) until the pH is neutral. The hydrolyzed extract was divided by adding 25 milliliters of ethyl acetate solvent to the bucket that had been separated and was already holding the hydrolyzed concentrated extract. After that, it was combined for 15 minutes and left to settle until two layers—the water phase on the bottom and the organic phase, or ethyl acetate, on top—formed. Until it lost its color, the researcher repeated the partitioning process with the same solvent. The % yield obtained was 5.6%

2.4.3. Sample Preparation for Analysis of Metabolite Profiling

Determination of the metabolite types of the ethyl acetate fraction of (*Chrysanthemum x morifolium* (Ramat.) Hemsl) leaves was performed using the UHPLC-HRMS instrument: LC (Thermo Scientific™ Vanquish™ UHPLC Binary Pump) and Orbitrap high-resolution mass spectrometry (Thermo Scientific™ Q Exactive™ Hybrid Quadrupole-Orbitrap™ High-Resolution Mass Spectrometer), column Thermo Scientific™ Accucore™ Phenyl-Hexyl 100 mm × 2.1 mm ID × 2.6 µm with three replications. Carefully weighed 10.00 mg of the ethyl acetate fraction of (*Chrysanthemum x morifolium* (Ramat.) Hemsl) leaves, then dissolved in methanol into a 10 mL volumetric flask and added microsyringe 3 µL. The mobile phases used were MS-grade water containing 0.1% formic acid (A) and MS-grade methanol containing 0.1% formic acid (B) employing a gradient technique with a flow rate of 0.3 mL/min. First, the mobile phase B was set at 5% and increased gradually to 90% in 16 min. Then, it was held at 90% for 4 min and continued to the initial condition (5% B) until 25 min. Data was obtained in the form of a chromatogram processed using the Compound Discovery 3 application. Hence, the data is in the way of peak area and m/z spectra of each detected peak and database mzCloud or https://www.chemspider.com/.

2.4.4. Cytotoxicity Test

2.4.4.1. Cell Line and Culture

The MCF-7 cell line was obtained from the Cellular and Molecular Biology Laboratory at Padjadjaran University, West Java, Indonesia's Faculty of Pharmacy. The cells were grown iDulbecco's's ModifieEagle's's Medium (DMEM). The cells were cultured in a humidified atmosphere at 37°C, under 5% CO_2, using an incubator (Thermo Scientific).

2.4.4.2. Preparation of Sample

Ethanol extract samples, ethyl acetate fractions and Cisplatin were weighed as much as 5 mg in a polytube, then dissolved in dimethyl sulfoxide (DMSO) (must not be more than 2%) as much as 100 µL, vortexed so that the sample was dissolved entirely then supplemented with complete growth media, then further dilutions were made until a test solution was obtained for ethanol extracts of concentrations (1,000; 500; 250; 125; 62.5; 31.25; 15.625; 7.813 ppm), ethyl acetate fraction concentrations (1,000; 500; 250; 125; 62.5; 31.25; 15.625; 7.813; 3.906 ppm) and cisplatin dilutions with concentrations (50; 25; 12.5; 6.25; 3.125; 1.56; 0.78125 ppm), then all dilutions were carried out using complete media.

2.4.4.3. Cytotoxicity Assay

The culture medium was removed and replaced with media containing anticancer drugs (Ethanol extract of concentrations (1,000; 500; 250; 125; 62.5; 31.25; 15.625; 7.813 ppm), ethyl acetate fraction concentrations (1,000; 500; 250; 125; 62.5; 31.25; 15.625; 7.813; 3.906 ppm), and cisplatin dilutions with concentrations (50; 25; 12.5; 6.25; 3.125; 1.56; 0.78125 ppm)) once MCF-7 cells had grown and seeded. The researcher added a 10µL WST-8 (Cell Counting Kit-8) dye to each well after the incubation period of 24 and 48 hours. After an hour, the plate was measured at 450 nm/655 nm with a microplate reader (Tecan nano quant infinite M200pro). The following formula was used to get the cell survival rate. With the use of GraphPad Prism 8, the IC_{50} value was determined by doing a linear regression analysis of the survival percentage versus medication concentration.

3. Results

The results obtained from the UHPLC-HRMS instrument are presented in the form of a chromatogram, where compounds that appear early in the chromatogram peak are polar and exhibit decreasing polarity in the subsequent peak. Then, the sample elutes from the column towards the MS detector. In this MS system, the analyte will go through three stages, namely the gas phase, the ion phase, and the separation of ions based on the ratio of mass to charge (m/z). The analyte in the form of a liquid will change into droplets through the needle and will be given a positive charge. Drops of analyte in the gas phase will evaporate the solvent through the spray before entering the capillary, so that solvent-free molecules are produced. Then the resulting ions will be separated. The detector will detect the results of the ion separation and will be displayed as a chromatogram (Figure 1). There is only one compound present for every peak on the chromatogram. After that, the chromatogram is analyzed using the Compound Discoverer 3.3 application to identify the m/z spectra and forecast the chemical formula of the interpreted compound. The name of the chemical is then looked for using the projected molecular formula, the mzCloud database, and the https://www.chemspider.com website. Following the acquisition of the compound's name and structure via the mzCloud database and website, the measured and calculated m/z values are compared using the ChemDraw tool to construct the

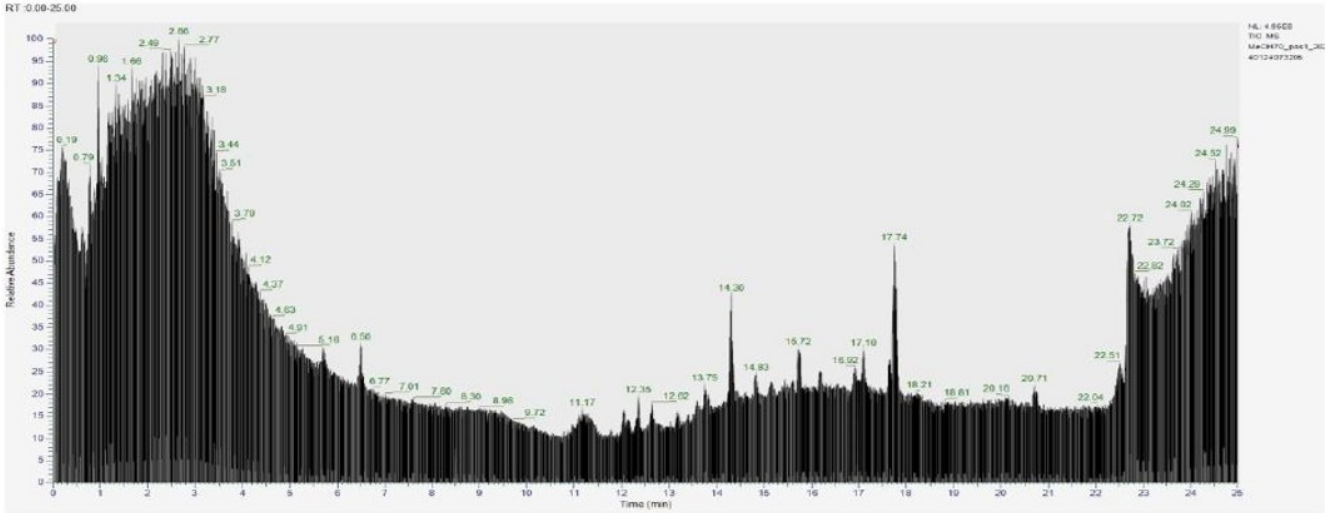

A

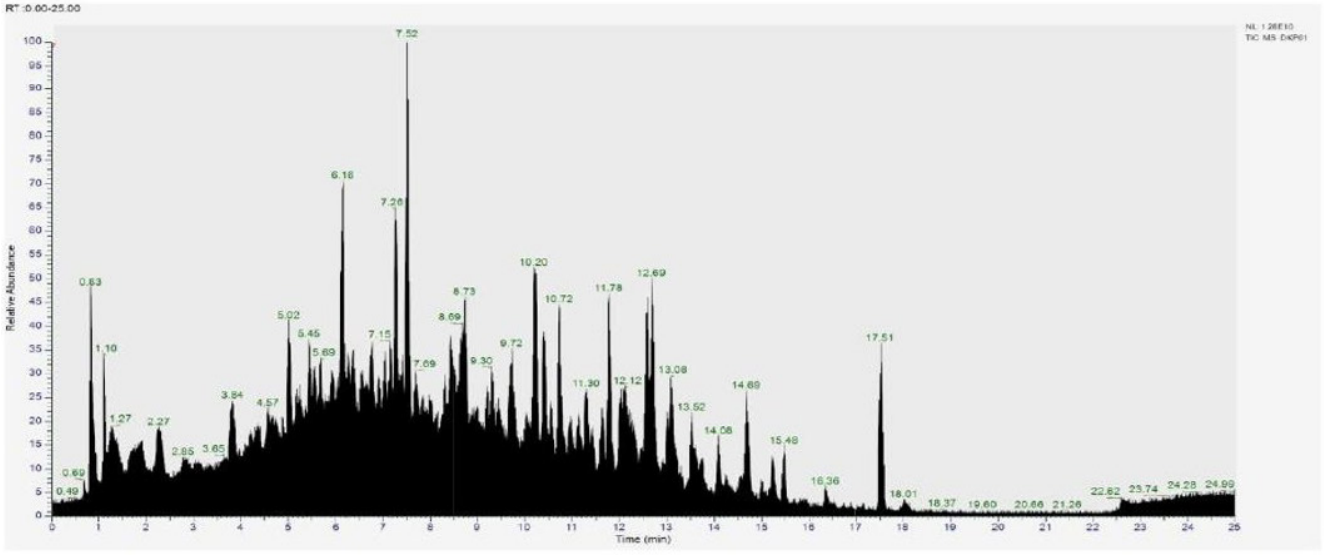

B

Figure 1. (A) Total ion chromatogram blank, (B) total ion chromatogram of ethyl acetate fraction of *C. morifolium* leaves

compound's structure. Figure 1 shows the blank's total ion chromatogram and the ethyl acetate fraction of (*Chrysanthemum x morifolium* (Ramat.) Hemsl) leaves. Based on the results of the interpretation of the chromatogram obtained for each peak, the predicted data for the Ethyl acetate fraction of (*Chrysanthemum x morifolium* (Ramat.) Hemsl) leaves, compound seen from the mzCloud Best Match, were more than 80%, 57 compounds were obtained as shown in Table 1. There are seven compounds in the ethyl acetate fraction of *Chrysanthemum x morifolium* (Ramat.) Hemsl leaves, which have the potential to act as anti-breast cancer (Table 2).

The cytotoxic test is an *in vitro* toxicity test that uses cells cultured in a medium to determine the antineoplastic activity of a compound on specific cancer cells and to assess the number of cell deaths using the IC_{50} parameter. Cytotoxicity test of (*Chrysanthemum*

Table 1. Metabolite profiling ethyl acetate fraction of *C. morifolium* leaves

Compound name	Retention time (min)	Area max	Mz cloud best match (%)	% Area	Fragmentation (m/z)
Dihydroartemisinin	5.302	124367627.2	84.4	0.141217865	$[M+H]^{+1}$ calcd for $C_{15}H_{22}O_5$, 282.14668; found, 283.15408
Scopoletin	5.907	718572035.1	97.5	0.815929443	$[M+H]^{+1}$ calcd for $C_{10}H_8O_4$, 192.04209; found, 193.04936
Esculetin	6.379	2315617119	97.4	2.629353904	$[M+H]^{+1}$ calcd for $C_9H_6O_4$, 178.02655; found, 179.03386
Kaempferol	7.781	4935953808	98.4	5.604713019	$[M+H]^{+1}$ calcd for $C_{15}H_{10}O_6$, 286.04756; found, 287.05478
Diosmetin	8.816	17535562290	98.7	19.91140883	$[M+H]^{+1}$ calcd for $C_{16}H_{12}O_6$, 300.06285; found, 301.07013
Chrysin	10.199	47569897.46	81.0	0.054015016	$[M+H]^{+1}$ calcd for $C_{15}H_{10}O_4$, 254.05771; found, 255.06499
Glycitein	10.321	27654762509	96.7	31.38782	$[M+H]^{+1}$ calcd for $C_{16}H_{12}O_5$, 284.06807; found, 285.07535
2-Amino-3,5,6-trimethyl-3,4-dihydropyridine-4-one	0.916	211525019	87.8	0.240183979	$[2M+H]^{+1}$ calcd for $C_7H_{11}N_3O$, 153.09025; found, 307.18735
Phenacetin	0.918	819348883.1	94.2	0.930360277	$[M+H]^{+1}$ calcd for $C_{10}H_{13}NO_2$, 179.0945; found, 180.10178; 162.09113 $[M+H-H_2O]^{+1}$; 212.12801 $[M+H+MeOH]^{+1}$
Adenine	0.921	9799900961	99.1	11.12766339	$[M+H]^{+1}$ calcd for $C_5H_5N_5$, 135.05434; found, 136.06161
6-Methylnicotinamide	1.16	18125937.87	90.5	0.020581773	$[M+H]^{+1}$ calcd for $C_7H_8N_0O$, 136.06371; found, 136.06161
Adenosine	1.194	46626240.38	98.2	0.052943505	$[M+H]^{+1}$ calcd for $C_{10}H_{13}N_5O_4$, 267.0967; found, 268.10394; 250.09323 $[M+H-H_2O]^{+1}$
5-amino-2-(dimethylamino) benzoic acid	1.374	43905697.65	93.0	0.049854363	$[M+H]^{+1}$ calcd for $C_9H_{12}N_2O_2$, 180.08983; found, 181.09720
2'-O-Methyladenosine	1.391	459183300.8	95.8	0.521396821	$[M+H]^{+1}$ calcd for $C_{11}H_{15}N_5O_4$, 281.11244; found, 282.11960
4-Methyl-5-thiazole-ethanol	1.486	114896821.2	96.7	0.521396821	$[M+H]^{+1}$ calcd for C_6H_9NOS, 143.04057; found, 144.04785
Dipropylene glycol	1.871	3582194342	99.6	4.067536294	$[M+H]^{+1}$ calcd for $C_6H_{14}O_3$, 134.09437; found, 135.10159; 152.12817$[M+NH_4]^{+1}$; 157.08365 $[M+Na]^{+1}$; 269.19586 $[2M+H]^{+1}$
Apocynin	1.933	70291717.49	81.4	0.079815355	$[M+H]^{+1}$ calcd for $C_9H_{10}O_3$, 166.06311; found, 167.07042
8-Hydroxyquinoline	3.442	1675936062	99.9	1.903004167	$[M+H]^{+1}$ calcd for C_9H_7NO, 145.0528; found, 146.06009
Esculin	4.038	53767096.02	99.8	0.061051856	$[M+H]^{+1}$ calcd for $C_{15}H_{16}O_9$, 340.07952; found, 341.06679
Caffeine	4.298	34027820.38	94.1	0.038638159	$[M+H]^{+1}$ calcd for $C_8H_{10}N_4O_2$, 194.0806; found, 195.08783

Table 1. Continued

Compound name	Retention time (min)	Area max	Mz cloud best match (%)	% Area	Fragmentation (m/z)
α-Pyrrolidinopropiophenone	4.454	44085513.12	93.2	0.050058542	$[M+H]^{+1}$ calcd for $C_{13}H_{17}NO$, 203.13112; found, 204.13834
Acetophenone	4.549	97135394.75	83.3	0.11029601	$[M+H]^{+1}$ calcd for C_8H_8O, 120.05763; found, 121.06492
2-Hydroxyquinoline	5.64	166337465.3	99.7	0.188874085	$[M+H]^{+1}$ calcd for C_9H_7NO, 145.05278; found, 146.05997; 187.06652 $[M+ACN+H]^{+1}$
Peruvinine	6.378	525431209	83.2	0.596620481	$[M+H]^{+1}$ calcd for $C_{15}H_{20}O_4$, 264.13615; found, 265.14349; 247.13283 $[M+H-H_2O]^{+1}$; 282.171 $[M+NH_4]^{+1}$
4-Indolecarbaldehyde	6.466	3830662103	99.2	4.349668289	$[M+H]^{+1}$ calcd for C_9H_7NO, 145.05269; found, 146.0599
Indole	6.467	313961467.4	98.0	0.356499269	$[M+H]^{+1}$ calcd for C_8H_7N, 117.05798; found, 118.06524
Apigetrin	6.628	292399918.9	99.9	0.332016404	$[M+H]^{+1}$ calcd for $C_{21}H_{20}O_{10}$, 432.10515; found, 433.11243
3',5,7-Trihydroxy-4'-methoxy flavanone	6.769	66353488.99	94.7	0.075343546	$[M+H]^{+1}$ calcd for $C_{16}H_{14}O_6$, 302.079; found, 303.06627
4-oxododecanedioic acid	6.973	81152200.41	85.7	0.092147295	$[M+H]^{+1}$ calcd for $C^{12}H^{20}O_5$, 244.13102; found, 245.13822; 227.12778 $[M+H-H_2O]^{+1}$
2,4-Dimethylbenzaldehyde	7.612	676125114.9	88.4	0.767731503	$[M+H]+1$ calcd for $C_9H_{10}O$, 134.07302; found, 135.08032; 117.07002 $[M+H-H_2O]^{+1}$
2-(3,4-dihydroxy phenyl)-5,7-dihydroxy-3,4-dihydro-2H-1-benzopyran-4-one	7.721	79117432.43	97.4	0.089836842	$[M+H]^{+1}$ calcd for $C_{15}H_{12}O_6$, 288.06343; found, 289.07071
3-(4-hydroxyphenyl)-7-methoxy-5-{[(3R,4S,5S,6R)-3,4,5-trihydroxy-6(hydroxymethyl)oxan-2-yl] oxy}-4H-chromene-4-one	7.957	5026393522	99.3	5.707406168	$[M+H]^{+1}$ calcd for $C_{22}H_{22}O_{10}$, 446.12102; found, 447.12830
Centaureidin	8.883	141082456.7	92.9	0.160197342	$[M+H]^{+1}$ calcd for $C_{18}H_{16}O_8$, 360.08421; found, 361.09143; 343.08057$[M+H-H_2O]^{+1}$
5,7-dihydrobenzo[d][1,3] benzodiazepin-6-one	9.211	221585116.1	90.6	0.251607092	$[M+H]+1$ calcd for $C_{13}H_{10}N_2O$, 210.07921; found, 211.08549
(-)-Caryophyllene oxide	9.796	1019454485	95.6	1.157577653	$[M+H]^{+1}$ calcd for $C_{15}H_{24}O$, 220.18248; found, 221.18965; 203.17909 $[M+H-H_2O]^{+1}$
1,4-dihydroxy-1,4-dimethyl-7-(propane-2-ylidene)-decahydroazulen-6-one	10.661	430587144.4	89.6	0.488926248	$[M+H]^{+1}$ calcd for $C_{15}H_{24}O_3$, 252.17247; found, 253.17981; 275.16205 $[M+Na]^{+1}$
4'-Methoxyacetophenone	10.664	37115365.96	83.8	0.042144028	$[M+H]^{+1}$ calcd for $C_9H_{10}O_2$, 150.0681; found, 151.07536
1,4-Bis(3,4,5-trimethoxyphenyl-hexahydrofuro[3,4c] furan	11.07	315130669.1	90.7	0.357826883	$[M+H]^{+1}$ calcd for $C_{24}H_{30}O8$, 446.1939; found, 447.20117; 429.19070 $[M+H-H_2O]^{+1}$; 464.22757 $[M+NH_4]^{+1}$
13-epi-12-oxo Phytodienoic Acid	11.976	687712649.6	96.3	0.780889001	$[M+H]+1$ calcd for $C_{18}H_{28}O_3$, 292.20379; found, 293.21109; 275.20065 $[M+H-H_2O]^{+1}$; 315.19159 $[M+Na]^{+1}$
4-(dimethylamino)-1,1-diphenylbut-3-en-2-one	12.192	66207352.67	83.0	0.07517761	$[M+H]^{+1}$ calcd for $C_{18}H_{19}NO$, 265.14662; found, 266.15384
Eicosapentaenoic acid	12.631	64943255.09	81.4	0.073742243	$[M+H]^{+1}$ calcd for $C_{20}H_{30}O_2$, 302.22418; found, 303.23154; 320.25732 [M+NH4]+1; 344.25793 $[M+ACN+H]^{+1}$

Table 1. Continued

Compound name	Retention time (min)	Area max	Mz cloud best match (%)	% Area	Fragmentation (m/z)
α-Eleostearic acid	12.684	2434283861	99.0	2.764098486	$[M+H]^{+1}$ calcd for $C_{18}H_{30}O$, 278.22405; found, 279.23129; 557.45532 $[2M+H]^{+1}$
3,5-di-tert-Butyl-4-hydroxybenzaldehyde	12.977	66507548.81	97.1	0.075518479	$[M+H]^{+1}$ calcd for $C_{15}H_{22}O_2$, 234.16197; found, 235.16925
Glycitin	13.343	33295912.68	98.7	0.037807087	$[M+H]^{+1}$ calcd for $C_{22}H_{22}O_{10}$, 446.12111; found, 447.12836
Kalecide	13.642	232406491.9	99.8	0.263894627	$[M+H]^{+1}$ calcd for $C_{16}H_{29}NO$, 251.22469; found, 252.23196
Linoleoyl Ethanolamide	13.887	72938867.11	81.4	0.08282116	$[M+H]^{+1}$ calcd for $C20H_{37}NO_2$, 323.28194; found, 324.28922
Palmitoyl ethanolamide	13.887	72938867.11	81.4	0.08282116	$[M+H]^{+1}$ calcd for $C_{18}H_{37}NO_2$, 299.28221; found, 300.28949
Oleoyl ethanolamide	14.327	15851110.15	98.5	0.017998735	$[M+H]^{+1}$ calcd for $C_{20}H_{39}NO_2$, 325.29781; found, 326.30508
Methyl alpha-eleostearate	14.703	81470519.36	96.9	0.092508743	$[M+H]^{+1}$ calcd for $C_{19}H_{32}O_2$, 292.23992; found, 293.24731
Palmitoleic acid	14,899	26771417.64	97.4	0,030398606	$[M+H]^{+1}$ calcd for $C_{16}H_{30}O_2$, 254.22438; found, 255.23175; 237.22116 $[M+H-H_2O]^{+1}$
Palmitoleic acid	14,899	26771417.64	97.4	0,030398606	$[M+H]^{+1}$ calcd for $C_{16}H_{30}O_2$, 254.22438; found, 255.23175; 237.22116 $[M+H-H_2O]^{+1}$
γ-Linolenic acid ethyl ester	14.936	32198669.29	87.3	0.036561181	$[M+H]^{+1}$ calcd for $C_{20}H_{34}O_2$, 306.25544; found, 307.26300; 339.28897 $[M+H-MeOH]^{+1}$
Oleamide	14.953	371669035.7	98.2	0.422025482	$[M+H]^{+1}$ calcd for $C_{18}H_{35}NO$, 281.27211; found, 282.27927
4-Methoxycinnamic acid	15.175	89804004.08	93.5	0.101971309	$[M+H]^{+1}$ calcd for $C_{10}H_{10}O_3$, 178.06301; found, 179.07022; 161.05971 $[M+H-H_2O]^{+1}$
Ethyl oleate	15.687	25299446.37	89.5	0.028727201	$[M+H]^{+1}$ calcd for $C_{20}H_{38}O_2$, 310.28682; found, 311.29410; 352.32047 $[M+ACN+H]+1$
Ethyl palmitoleate	15,772	21722250.99	84.4	0.024665341	$[M+H]^{+1}$ calcd for $C_{18}H_{34}O_2$, 282.25548; found, 283.26294
Alverine	16.054	9849194.473	87.0	0.011183636	$[M+H]^{+1}$ calcd for $C_{20}H_{27}N$, 281.21416; found, 282.22159
Methyl palmitate	17.215	19864157.25	93.1	0.022555499	$[M+H]^{+1}$ calcd for $C_{17}H_{34}O_2$, 270.25582; found, 271.26309

Table 2. Spectra m/z and structure compound of ethyl acetate fraction of C.morifolium leaves that have the potential as breast anticancer

Compound name	Molecule	Spectra m/z and structure
Glycitein	$C_{16}H_{12}O_5$	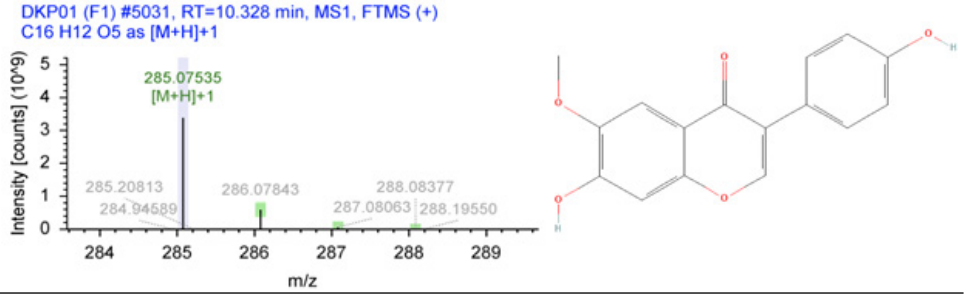

Table 2. Continued

Compound name	Molecule	Spectra m/z and structure
Diosmetin	$C_{16}H_{12}O_6$	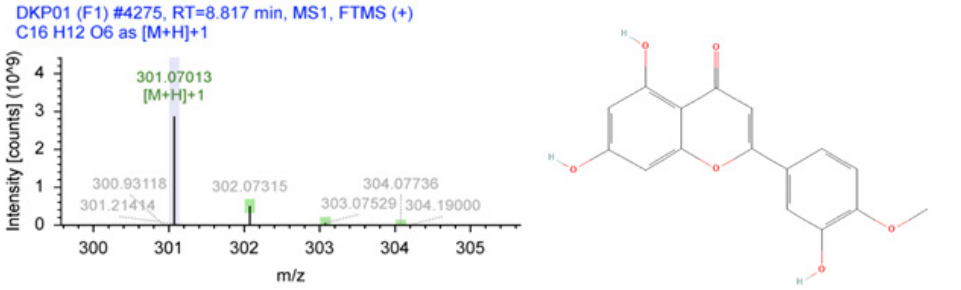
Kaempferol	$C_{15}H_{10}O_6$	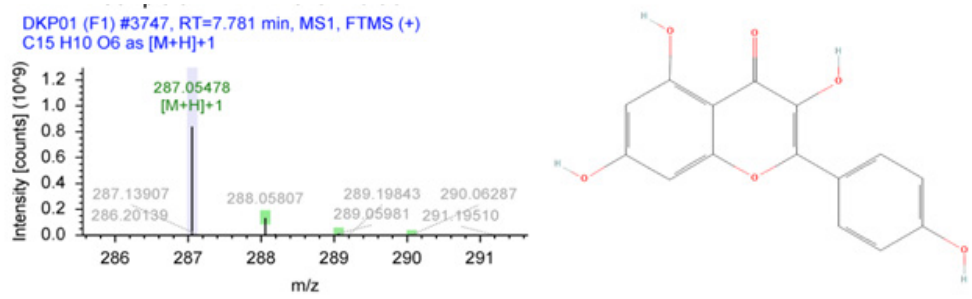
Esculetin	$C_9H_6O_4$	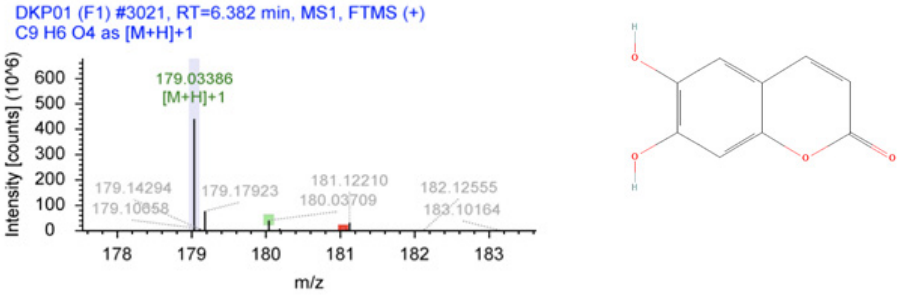
Scopoletin	$C_{10}H_8O_4$	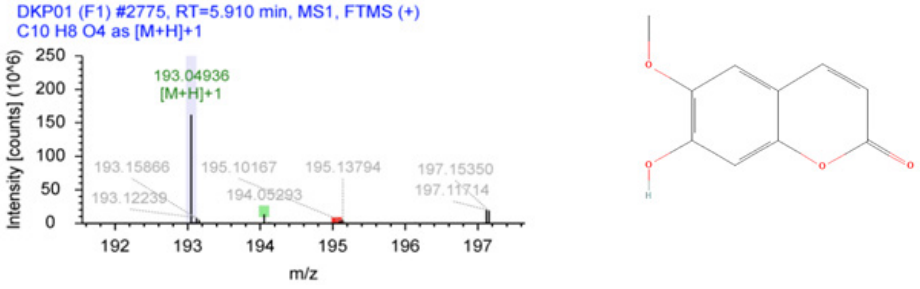
Dyhidroartemisinin	$C_{15}H_{22}O_5$	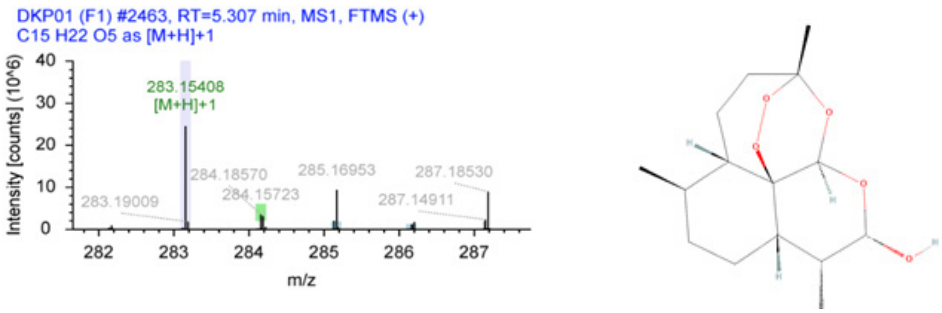

Table 2. Continued

Compound name	Molecule	Spectra m/z and structure
Chrysin	$C_{15}H_{10}O_4$	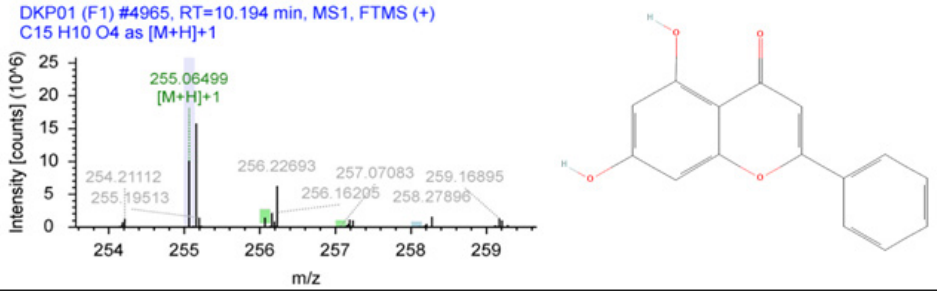

x morifolium (Ramat.) Hemsl leaves ethanol extract against MCF-7 cancer cells using the WST-8 test method. The test data were obtained as absorbance data, and the concentration's percentage concentration of live cells was calculated. The graph of the relationship between % living cells and the concentration of ethanol extract, ethyl acetate fraction, and Cisplatin is presented in Figures 2 and 3. This data was then analyzed using GraphPad Prism 8 to calculate the IC_{50} value. Data from observation of the cytotoxicity test of the ethanol extract and ethyl acetate fraction of (*Chrysanthemum x morifolium* (Ramat.) Hemsl leaves at 24-hour and 48-hour incubation are presented in Tables 3 and 4.

4. Discussion

The Chrysanthemum plant (*Chrysanthemum x morifolium* (Ramat.) Hemsl is one of the medicinal ingredients that has been used for a long time in traditional medicine. In its development, it is hoped that other parts of the Chrysanthemum plant, such as *Chrysanthemum x morifolium* (Ramat.) Hemsl leaves can be used as raw materials for traditional medicine.

Metabolite profiling aims to determine the compound content in the ethyl acetate fraction of (*Chrysanthemum x morifolium* (Ramat.) Hemsl leaves. Metabolite profiling analysis using UHPLC/HRMS instruments. This method serves to clarify the structure of different compounds by offering rapid chromatography, enhanced separation, short chromatography run times, excellent sensitivity and selectivity, precise measurements, and reliable fragmentation (Ma *et al.* 2022).

A total of 57 phytochemical compounds (Table 1) were analyzed in the ethyl acetate fraction of *Chrysanthemum x morifolium* (Ramat.) Hemsl leaves. There has not been much research on the isolation of *Chrysanthemum morifolium* leaves. In another study, six sesquiterpene compounds were found in the stems and leaves of *Chrysanthemum morifolium* Ramat (Zhang *et al.* 2023). From several previous studies, the isolation of compounds that were mostly done on the flower part. The compounds that have been found are chrysanthelignanoside A, chrysanthelignanoside B, 2,6-dimethoxyl-4-hydroxymethyl-phenol 1-O-(6-O-caffeoyl)-β-D-glucopyranoside, ethylene glycol 1-O-(6-O-caffeoyl)-β-D-glucopyranoside, (2S)-propane-1,2-diol 1-O-(6-O-caffeoyl)-β-D-glucopyranoside, and butane-2,3-diol 2-O-(6-O-caffeoyl)-β-D-glucopyranoside (Yang *et al.* 2018). Another study found two new caffeoylquinic acid derivatives, a new flavanone glycoside, and six flavanone glycosides, including eriodictyol, eriodictyol 7-O-β-D-glucopyranoside, eriodictyol 7-O-β-D-glucuronide, eriodictyol 7-O-β-D-rutinoside, hesperetin 7-O-β-D-glucuronide, and dehydrokaempferide Ramat (Yang *et al.* 2019). A new endoperoxysquiterpene lactone, 10α-hydoxy-1α,4α-endoperoxy-guaia-2-en-12,6α-olide, flavanone eriodictyol, flavone glycosides acacetin-7-O-β-D-glucopyranoside and acacetin-7-O-α-L-rhamopyranoside (Luyen *et al.* 2013). From the roots of Chrysanthemum morifolium, a total of 20 terpenoids were detected, including four monoterpenes, 15 sesquiterpenes, and one diterpene (Zhang *et al.* 2020).

The metabolite profiling results using UHPLC/HRMS on the ethyl acetate fraction (*Chrysanthemum x morifolium* (Ramat.) Hemsl shows that the ethyl acetate fraction contains the largest number of main

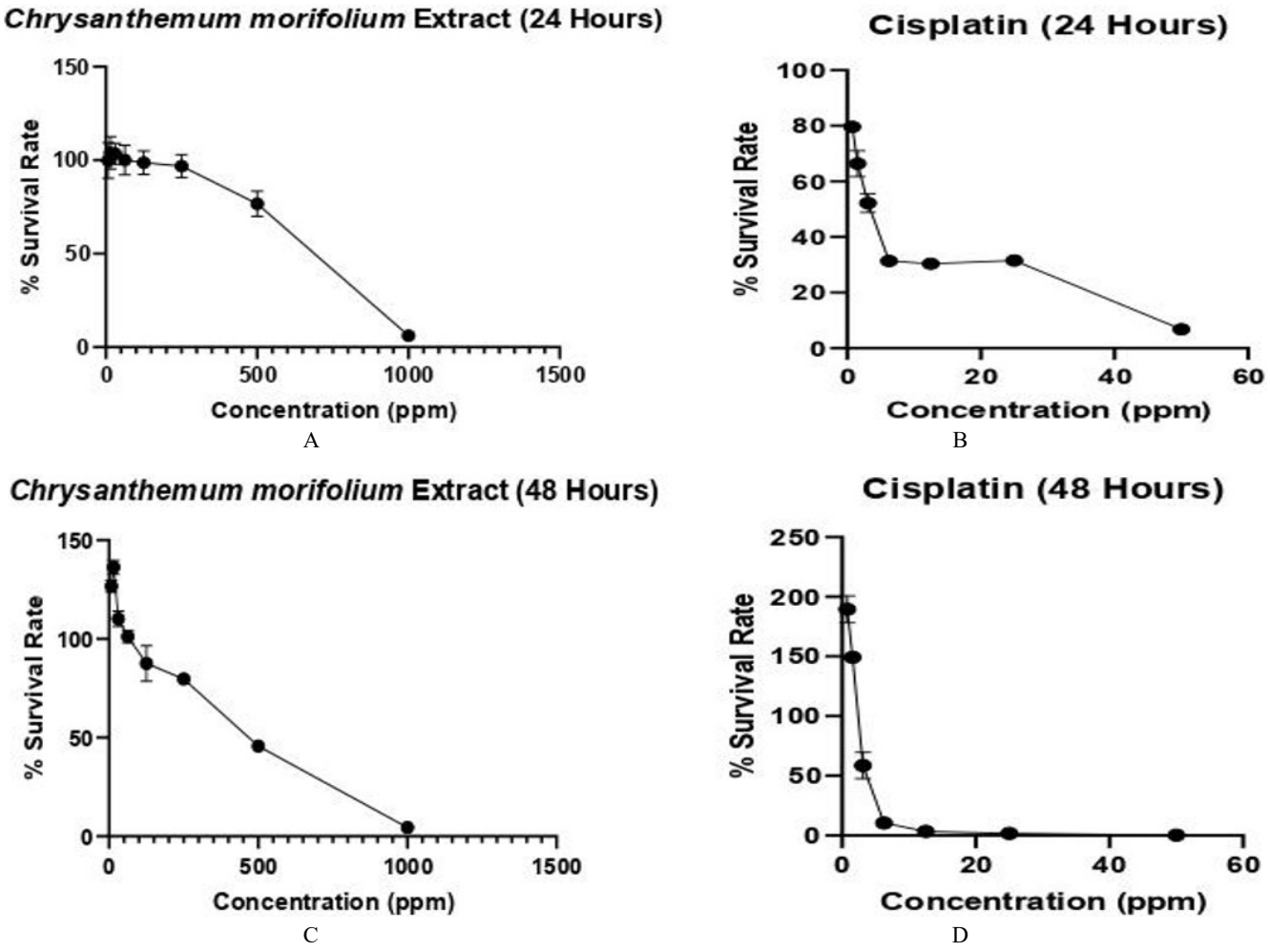

Figure 2. Graph of the relationship between the % survival rate and concentration with three repetitions (A) ethanol extract 24 hours, (B) cisplatin 24 hours, (C) ethanol extract 48 hours, (D) cisplatin 48 hours

compounds, namely glycitein with a % area of 31.39%. Apart from that, there are other compounds such as diosmetin (19.91%), kaempferol (5.61%), esculetin (2.63%), scopoletin (0.82%), dihydroartemisinin (0.14%), and Chrysinn (0.05%), which is a flavonoid compound and has the potential to act as an anti-breast cancer agent, as shown in Table 2. Previous studies demonstrated that glycitein has a positive effect on MCF-7 cell migration. Diosmetin inhibits the growth of MDA-MB-231 cells and promotes apoptosis by activating the intrinsic mitochondrial apoptotic pathway, accumulating ROS, and causing cell cycle arrest. Kaempferol can inhibit MCF-7 cell activity. Esculetin, a naturally occurring coumarin molecule, causes Ca (2+) to travel and activates mitochondrial apoptotic pathways linked to Ca (2+) that induce cell cycle arrest in human breast cancer cells ZR-75-1. Scopoletin can inhibit MDA-MB-231. Dihydroartemisinin reduces TGF-β1 signaling-related CIZ1 expression, preventing breast cancer carcinogenesis and metastasis. Chrysin inhibits the growth of breast cancer cells by inducing cancer cell apoptosis (Zhang *et al.* 2015; Chang *et al.* 2016; Samarghandian *et al.* 2016; Yi *et al.* 2016; Zhong *et al.* 2016; Lee *et al.* 2017; Choi *et al.* 2019; Zang *et al.* 2019; Zhu and Xue 2019; Wang *et al.* 2019, 2022; Kamran *et al.* 2022). Flavonoid compounds have been reported to have antiproliferative effects on breast cancer cells and can induce cell apoptosis (Jeong Choi and Shick Ahn 2008; Sun *et al.* 2015; Yi *et al.* 2016; Vrhovac Madunić *et al.* 2018; Abotaleb *et al.* 2019).

The IC_{50} value is an in vitro concentration that can inhibit/inhibit breast cancer cell activity by 50%. A reduced IC_{50} value indicates that the substance may be utilized as a stand-in for a more effective anticancer medication since it requires a small dose of 50% to impede cancer cell proliferation activity. Ichemical's IC_{50} value is less than 100 ppm, it is considered to

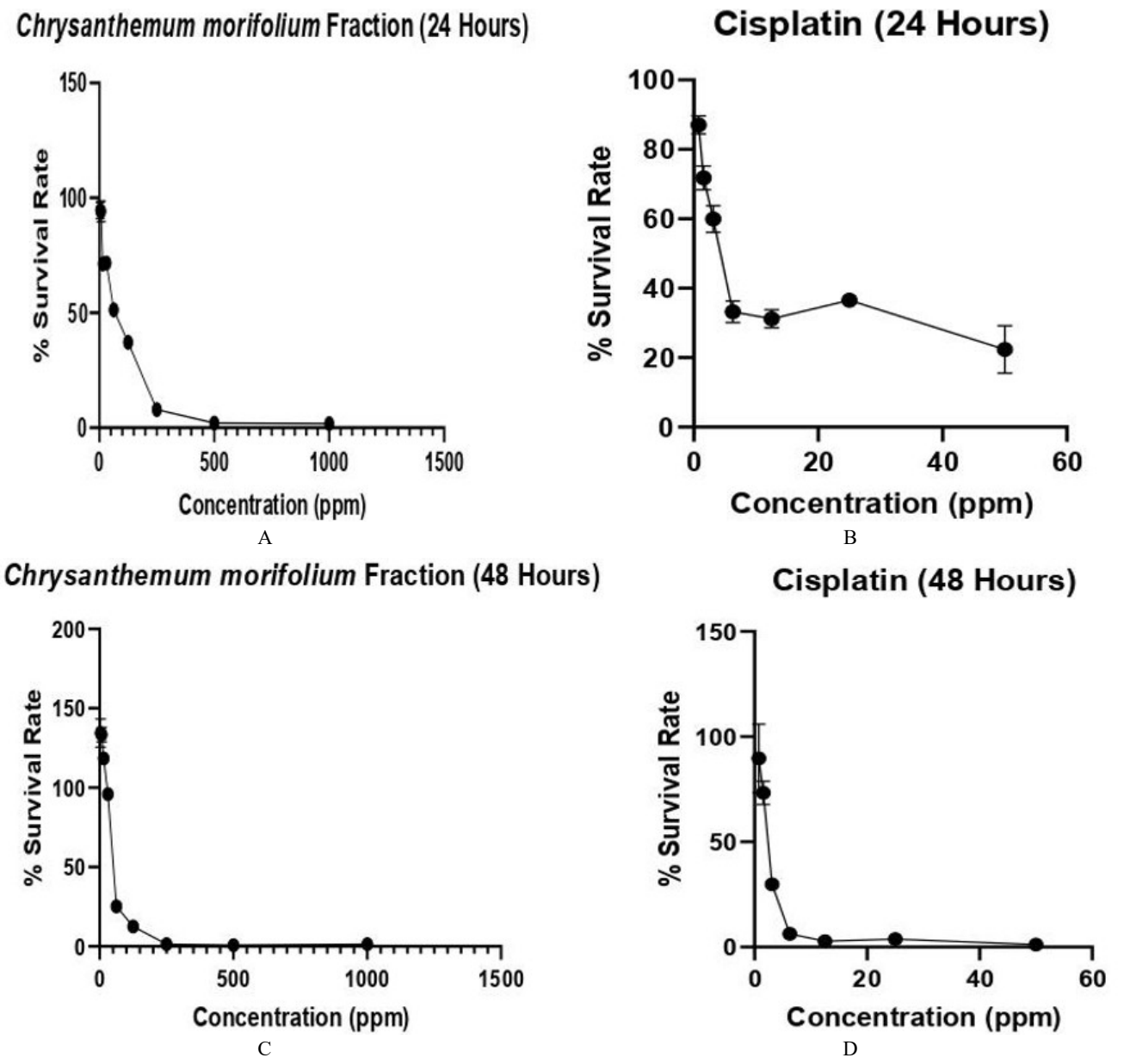

Figure 3. Graph of the relationship between % survival rate and concentration with three repetitions (A) ethyl acetate fraction 24 hours, (B) cisplatin 24 hours, (C) ethyl acetate 48 hours, (D) cisplatin 48 hours

Table 3. IC_{50} value of *C. morifolium* leaves extract (CMLE) and cisplatin

Sample	IC_{50} (ppm)		Cytotoxic activity
	24 hours	48 hours	
CMLE	564	208	Moderate
CISPLATIN	5,519	2.41	Potential

Table 4. IC_{50} value of ethyl acetate fraction of *C. morifolium* leaves (EFCML) and cisplatin

Sample	IC_{50} (ppm)		Cytotoxic activity
	24 hours	48 hours	
EFCML	66.31	40.35	Moderate
CISPLATIN	3,442	2,246	Potential

be a potentially cytotoxic compound; if it is between 100 and 1,000 ppm, it is considered to have moderate cytotoxic activity; and if it is greater than 1,000 ppm, it is considered to have no cytotoxic activity (Prayong *et al.* 2008). The IC_{50} value of the ethanol extract of (*Chrysanthemum x morifolium* (Ramat.) Hemsl leaves in the 100-500 ppm range have moderate cytotoxic activity.

Meanwhile, the ethyl acetate fraction of (*Chrysanthemum x morifolium* (Ramat.) Hemsl leaves in the 100-10 ppm range have potential cytotoxic activity. The IC_{50} value of the ethanol extract of *Chrysanthemum x morifolium* (Ramat.) Hemsl leaves in the range of 100-500 ppm have moderate cytotoxic activity. Meanwhile, the ethyl acetate fraction of *Chrysanthemum x morifolium* (Ramat.) Hemsl leaves in the range of 100-10 ppm have potential cytotoxic activity. Ethanol extract and ethyl acetate fraction of *Chrysanthemum x morifolium* (Ramat.) Hemsl leaves have less potent cytotoxic activity when compared to Cisplatin as a positive control, with an IC_{50} value below 10 ppm, and very potent cytotoxic activity. In previous studies, the compounds rutin, luteolin, quercetin, and apigenin in Chrysanthemum morifolium flowers had anti-breast cancer activity in MCF-7 cells (Hodaei *et al.* 2021a).

As an initial finding, the results of the cytotoxicity test of the ethyl acetate fraction containing flavonoids on MCF-7 cells *in vitro* showed potential cytotoxic activity. Further studies are needed to confirm the anticancer potential and explore applications in the field of human health. This result is in line with several studies that show that flavonoids have strong anticancer potential in various types of cancer (Ahmed *et al.* 2016; Zheng *et al.* 2016; Sheng 2020; Liu *et al.* 2021b, 2021a). The mechanism behind the anticancer activity of flavonoids involves inducing apoptosis, autophagy, and cell cycle arrest, as well as inhibiting proliferation and reducing cancer cell invasion (Boik 2001). In addition, flavonoids regulate cancer-related signaling pathways (Bishayee *et al.* 2011; Kalia *et al.* 2016).

This study has some limitations. It was restricted to metabolite profiling of the ethyl acetate fraction of *Chrysanthemum morifolium* leaves and cytotoxicity evaluation only against MCF-7 breast cancer cells. No normal cell line was included as a control, and no further mechanistic studies, such as apoptosis, cell cycle analysis, or gene expression, were performed. Therefore, the findings cannot be directly extrapolated to *in vivo* conditions. Future studies should focus on the isolation and characterization of the active compounds, elucidation of their molecular mechanisms, and validation through *in vivo* models.

In conclusion, the results of metabolite profiling using UHPLC-HRMS on the Ethyl acetate fraction of (*Chrysanthemum x morifolium* (Ramat.) Hemsl.) leaves contained seven compounds that have the potential for anti-breast cancer activity, such as glycitein, diosmetin, kaempferol, esculetin, scopoletin, dihydroartemisinin, and Chrysinin with successive percentages of 31.39%, 19.91%, 5.61%, 2.63%, 0.82%, 0.14% and 0.05%. The ethyl acetate fraction of (*Chrysanthemum x morifolium* (Ramat.) Hemsl.) leaves has higher cytotoxic activity than the extract. The ethyl acetate fraction had cytotoxic activity for MCF-7 with IC_{50} values of 66.31 ppm at 24-hour incubation and 40.35 ppm at 48-hour incubation.

Acknowledgements

This research was funded by the Directorate of Research and Community Service, Ministry of Research, Technology, and Higher Education of Indonesia under the Doctoral Dissertation Research Scheme (2023). This study did not involve human participants or animal experiments. The MCF-7 breast cancer cell line used in this study is a commercially available established cell line, which was obtained from the Translational Pharmacy Research Laboratory, Faculty of Pharmacy, Universitas Padjadjaran, Indonesia. Therefore, ethical approval was not required.

References

Abotaleb, M., Samuel, S.M., Varghese, E., Varghese, S., Kubatka, P., Liskova, A., Büsselberg, D., 2019. Flavonoids in cancer and apoptosis. *Cancers.* 11, 28. https://doi.org/10.3390/cancers11010028

Ahmed, S.I., Hayat, M.Q., Tahir, M., Mansoor, Q., Ismail, M., Keck, K., Bates, R.B., 2016. Pharmacologically active flavonoids from the anticancer, antioxidant, and antimicrobial extracts of *Cassia angustifolia* Vahl. *BMC Complementary and Alternative Medicine.* 16, 1–9. https://doi.org/10.1186/s12906-016-1443-z

Bishayee, A., Ahmed, S., Brankov, N., Perloff, M., 2011. Triterpenoids as potential agents for the chemoprevention and therapy of breast cancer. *Frontiers in Bioscience.* 16, 980–996. https://doi.org/10.2741/3730

Boik, J., 2001. 15 Natural compounds in cancer therapy. *International Journal of Pharmaceutical Medicine.* 15, 256. https://doi.org/10.2165/00124363-200110000-00017

[BPS] Badan Pusat Statistik Indonesia, 2022. Produksi Tanaman Florikultura (Hias)., 2022. Available at: https://www.bps.go.id/indicator/55/64/1/produksi-tanaman-florikultura-hias-.html. [Date accessed: 9 June 2023]

Bray, F., Ferlay, J., Soerjomataram, I., Siegel, R.L., Torre, L.A., Jemal, A., 2018. Global cancer statistics 2018: GLOBOCAN estimates of incidence and mortality worldwide for 36 cancers in 185 countries. *CA: A Cancer Journal for Clinicians.* 68, 394–424. https://doi.org/10.3322/caac.21492

Cai, W., Xiong, Y., Han, M., Li, Z., Peng, L., Zhang, H., Zou, Q., Wu, L., Ye, Q., Liao, L., 2021. Characterization and quantification of luteolin-metal complexes in aqueous extract of lonicerae japonicae flos and huangshan wild Chrysanthemum. *International Journal of Analytical Chemistry.* 2021, 1-9. https://doi.org/10.1155/2021/6677437

Chang, H.T., Chou, C.T., Lin, Y.S., Shieh, P., Kuo, D.H., Jan, C.R., Liang, W.Z., 2016. Esculetin, a natural coumarin compound, evokes Ca2+ movement and activation of Ca2+-associated mitochondrial apoptotic pathways that involved cell cycle arrest in ZR-75-1 human breast cancer cells. *Tumor Biology.* 37, 4665–4678. https://doi.org/10.1007/s13277-015-4286-1

Choi, J., Lee, D.H., Park, S.Y., Seol, J.W., 2019. Diosmetin inhibits tumor development and block tumor angiogenesis in skin cancer. *Biomedicine and Pharmacotherapy.* 117, 109091. https://doi.org/10.1016/j.biopha.2019.109091

Dermawan, D., Sumirtanurdin, R., Dewantisari, D., 2019. Molecular dynamics simulation of estrogen receptor alpha against andrografolid as anti breast cancer. *IJPST.* 6, 65-76.

Hodaei, M., Rahimmalek, M., Behbahani, M., 2021a. Anticancer drug discovery from Iranian *Chrysanthemum cultivars* through system pharmacology exploration and experimental validation. *Scientific Reports.* 11, 1–11. https://doi.org/10.1038/s41598-021-91010-y

Hodaei, M., Rahimmalek, M., Arzani, A., 2021b. Variation in bioactive compounds, antioxidant and antibacterial activity of Iranian *Chrysanthemum morifolium* cultivars and determination of major polyphenolic compounds based on HPLC analysis. *Journal of Food Science and Technology.* 58, 1538–1548. https://doi.org/10.1007/s13197-020-04666-1

Jeong Choi E, Shick Ahn W., 2008. 2 Kaempferol induced the apoptosis via cell cycle arrest in human breast cancer MDA-MB-453 cells. *Nutr Res Pract.* 2, 322-325.

Kalia, R., Katnoria, J.K., Nagpal, A.K., 2016. Antitumor activity of aqueous leaf extracts of different cultivars of *Chrysanthemum morifolium* R. using potato disc tumor assay. *Journal of Pharmaceutical Sciences and Research.* 8, 1262–1265.

Kamran, S., Sinniah, A., Chik, Z., Alshawsh, M.A., 2022. Diosmetin exerts synergistic effects in combination with 5-fluorouracil in colorectal cancer cells. *Biomedicines.* 10, 531. https://doi.org/10.3390/biomedicines10030531

Kemenkes RI., 2019. Riskesdas 2018. Kementerian Kesehatan RI 1, 1.

Lee, G.A., Choi, K.C., Hwang, K.A., 2017. Kaempferol, a phytoestrogen, suppressed triclosan-induced epithelial-mesenchymal transition and metastatic-related behaviors of MCF-7 breast cancer cells. *Environmental Toxicology and Pharmacology.* 49, 48–57. https://doi.org/10.1016/j.etap.2016.11.016

Lestari, N.A., Irawati, S., Listiyana, A., Indrawijaya, Y.Y.A., Annisa, R., Bhagawan, W.S., Mutiah, R., 2019. Anticancer activities and metabolite fingerprinting of uplc-qtof-ms/ms method from *Chrysanthemum cinerariifolium* (Trev). *Journal of Islamic Pharmacy.* 4, 19. https://doi.org/10.18860/jip.v4i1.7728

Liu, L.F., Sun, H.H., Tan, J.B., Huang, Q., Cheng, F., Xu, K.P., Zou, Z.X., Tan, G.S., 2021a. New cytotoxic biflavones from *Selaginella doederleinii. Natural Product Research.* 35, 930–936. https://doi.org/10.1080/14786419.2019.1611813

Liu, W.H., Huang, D.H., Gan, K., Wang, S.T., 2021b. Saniculamin C, a new flavonoid from *Sanicula lamelligera. Journal of Asian Natural Products Research.* 23, 379–384. https://doi.org/10.1080/10286020.2020.1730332

Liu, Y.H., Mou, X., Zhou, D.Y., Zhou, D.Y., Shou, C.M., 2018. Extraction of flavonoids from *Chrysanthemum morifolium* and antitumor activity *in vitro. Experimental and Therapeutic Medicine.* 15, 1203–1210. https://doi.org/10.3892/etm.2017.5574

Luyen, N.T., Tram, L.H., Hanh, T.T.H., Binh, P.T., Dang, N.H., Minh, C.V., Dat, N.T., 2013. Inhibitors of α-glucosidase, α-amylase, and lipase from *Chrysanthemum morifolium. Phytochemistry Letters.* 6, 322-325. http://doi.org/10.1016/j.phytol.2013.03.015

Ma, D., Kanisha Chelliah, C., Alharbi, N.S., Kadaikunna, S., Khaled, J.M., Alanzi, K.F., Manoharan, N., Rajivgandhi, G., 2021. *Chrysanthemum morifolium* extract mediated Ag NPs improved the cytotoxicity effect in A549 lung cancer cells. *Journal of King Saud University - Science.* 33, 101269. https://doi.org/10.1016/j.jksus.2020.101269

Ma, J., Li, K., Shi, S., Li, J., Tang, S., Liu, L.H.., 2022. The application of UHPLC-HRMS for quality control of traditional Chinese medicine. *Frontiers in Pharmacology.* 13, 1–10. https://doi.org/10.3389/fphar.2022.922488

Matsumura, S., Ohta, T., Yamanouchi, K., Liu, Z., Sudo, T., Kojimahara, T., Seino, M., Narumi, M., Tsutsumi, S., Takahashi, T., Takahashi, K., Kurachi, H., Nagase, S., 2017. Activation of estrogen receptor α by estradiol an Cisplatinin induces platinum-resistance in ovarian cancer cells. *Cancer Biology and Therapy.* 18, 730–739. https://doi.org/10.1080/15384047.2016.1235656

Muchtaridi, M., Syahidah, H.N., Subarnas, A., Yusuf, M., Bryant, S.D., Langer, T., 2017. Molecular docking and 3D-pharmacophore modeling to study the interactions of chalcone derivatives with estrogen receptor alpha. *Pharmaceuticals.* 10, 1–12. https://doi.org/10.3390/ph10040081

bin Muhamad Noor, M.T., Mohd Zainuddin, H.Z.binti, Bin Abdul Aziz, M.Y., Bin Tuan Johari, S.A.T., Binti Wan Osman, W.N., 2021. Cytotoxicity effect and morphological changes of *Chrysanthemum morifolium* methanolic extract against chronic myeloid leukaemia K-562 cell line. *Asian Journal of Medicine and Biomedicine.* 5, 22–28. https://doi.org/10.37231/ajmb.2021.5.s1.446

Mutiah, R., Yen, Y., Indrawijaya, A., Puspita, D., 2020a. Study *in silico* compounds in 96% ethanol extract of *Chrysanthemum cinerariifolium* (Trev.) leaves towards alfa estrogen receptors. *Indonesian Journal of Cancer Chemoprevent.* 11, 144–153.

Mutiah, R., Inayatin, A.L., Annisa, R., Indrawijaya, Y.Y.A, Listiyana A., 2020b. Inhibition of cell cycle and induction of apoptosis y ethanol leaves extract of *Chrysanthemum cinerariifolium* (Trev.) in T47D breast cancer cells. *Indonesian Journal of Pharmacy.* 31, 1–10. https://doi.org/10.14499/indonesianjpharm31iss1pp1

Mutiah, R., Yen, Y., Indrawijaya, A., Puspita, D., Kumala, R.R., Hamid, H.A., 2021. Prediction of anti-sar-cov-2 activity from *Chrysanthemum cinerariifolium* (Trev.) compounds. *Solid State Technology.* 64, 4840–4849.

Obakan-yerlikaya, P., Damla, E., Coker-gurkan, A., 2017. *Breast Cancer and Flavonoids as Treatment Strategy Breast Cancer and Flavonoids as Treatment Strategy*. IntechOpen, London. http://doi.org/10.5772/66169

Park, K.H., Yang, M.S, Park, M.K., Kim, S.C., Yang, C.H., Park, S.J., Lee, J.R., 2009. A new cytotoxic guaianolide from *Chrysanthemum boreale. Fitoterapia.* 80, 54–56. https://doi.org/10.1016/j.fitote.2008.09.013

Prayong, P., Barusrux, S., Weerapreeyakul, N., 2008. Cytotoxic activity screening of some indigenous Thai plants. *Fitoterapia.* 79, 598–601. https://doi.org/10.1016/j.fitote.2008.06.007

Samarghandian, S, Azimi-Nezhad, M., Borji, A., Hasanzadeh, M., Jabbari, F., Farkhondeh, T., Samini, M., 2016. Inhibitory and cytotoxic activities oChrysinin on human breast adenocarcinoma cells by induction of apoptosis. *Pharmacognosy Magazine.* 12, 436–440. https://doi.org/10.4103/0973-1296.191453

Sheng ZZ., 2020. Anticancer effects of catechin flavonoid in human glioma cells are mediated via autophagy induction, cell cycle arrest, inhibition of cell migration and invasion and targeting MAPK/ ERK signalling pathway. *Journal of B.U.ON.* 25, 1084–1090.

Siegel, R.L, Miller, K.D., Wagle, N.S., Jemal, A., 2023. Cancer statistics, 2023. *CA: A Cancer Journal for Clinicians.* 73, 17–48. https://doi.org/10.3322/caac.21763

Sun, D.W., Zhang, H.Da., Mao, L., Mao, C.F., Chen, W., Cui, M., Ma, R., Cao, H.X., Jing, C.W., Wang, Z., Wu, J.Z., Tang, J.H., 2015. Luteolin inhibits breast cancer development and progression *in vitro* and *in vivo* by suppressing notch signaling and regulating MiRNAs. *Cellular Physiology and Biochemistry.* 37, 1693–1711. https://doi.org/10.1159/000438535

Sung, H., Ferlay, J., Siegel, R.L., Laversanne, M., Soerjomataram, I., Jemal, A., Bray, F., 2021. Global cancer statistics 2020: GLOBOCAN estimates of incidence and mortality worldwide for 36 cancers in 185 countries. *CA: A Cancer Journal for Clinicians.* 71, 209–249. https://doi.org/10.3322/caac.21660

Vrhovac Madunić, I., Madunić, J., Antunović, M., Paradžik, M., Garaj-Vrhovac, V., Breljak, D., Marijanović, I., Gajski, G., 2018. Apigenin, a dietary flavonoid, induces apoptosis, DNA damage, and oxidative stress in human breast cancer MCF-7 and MDA MB-231 cells. *Naunyn-Schmiedeberg'se, rg's Archives of Pharmacology.* 391, 537–550. https://doi.org/10.1007/s00210-018-1486-4

Wang, C., Li, S., Ren, H., Sheng, Y., Wang, T., Li, M., Zhou, Q., He, H., Liu, C., 2019. Anti-proliferationion and pro-apoptotic effects of diosmetin via modulating cell cycle arrest and mitochondria-mediated intrinsic apoptotic pathway in MDA-MB-231 cells. *Medical Science Monitor.* 25, 4639–4647. https://doi.org/10.12659/MSM.914058

Wang, J., Ma, S., Li, L., Chen, Y., Yang, Q., Wang, F., Zheng, M., Miao, S., Shi, X., 2022. Investigation into the *in vivo* mechanism of diosmetin in patients with breast cancer and COVID-19 using bioinformatics. *Frontiers in Pharmacology.* 13, 1–12. https://doi.org/10.3389/fphar.2022.983821

Xie, Y.Y., Yuan, D., Yang, J.Y., Wang, L.H., Wu, C.F., 2009. Cytotoxic activity of flavonoids from the flowers of *Chrysanthemum morifolium* on human colon cancer colon205 cells. *Journal of Asian Natural Products Research.* 11, 771–778. https://doi.org/10.1080/10286020903128470

Yang, P.F., Yang, Y.N., Feng, Z.M., Jiang, J.S., Zhang, P.C., 2018. Six new compounds from the flowers of *Chrysanthemum morifolium* and their biological activities. *Bio-Organic Chemistry.* 82, 139-144. https://doi.org/10.1016/j.bioorg.2018.10.007

Yang, P.F., Yang, Y.N., He, C.Y., Chen, J.F., Yuan, Q.S., Zhao, S.C., Fu. Y.F., Zhang, P.C., Mao, D.B., 2019. New caffeoylquinic acid derivatives and flavanone glycoside from the flowers of *Chrysanthemum morifolium* and their bioactivities. *Molecules.* 24, 850. https://doi.org/10.3390/molecules24050850

Yi, X., Zuo, J., Tan, C., Xian, S., Luo, C., Chen, S., Yu, L., Luo, Y., 2016. Kaempferol, a flavonoid compound from *Gynura medica* induced apoptosis and growth inhibition in MCF-7 breast cancer cells. *African Journal of Traditional, Complementary and Alternative Medicines.* 13, 210–215. https://doi.org/10.21010/ajtcam.v13i4.27

Zang, Y.Q., Feng, Y.Y., Luo, Y.H., Zhai, Y.Q., Ju, X.Y., Feng, Y.C., Wang, J.R., Yu, C.Q., Jin, C.H., 2019. Glycitein induces reactive oxygen species-dependent apoptosis and G0/G1 cell cycle arrest through the MAPK/STAT3/NF-κB pathway in human gastric cancer cells. *Drug Development Research.* 80, 573–584. https://doi.org/10.1002/ddr.21534

Zhang, B., Su, J.P., Bai, Y., Li, J., Liu, Y.H., 2015. Inhibitory effects of O-methylated isoflavone glycitein on human breast cancer SKBR-3 cells. *International Journal of Clinical and Experimental Pathology.* 8, 7809–7817.

Zhang, K., Jiang, Y., Zhao, H., Kolnerr, T.G., Chen, S., Chen, F.C., Chen, F., 2020. Diverse terpenoids and their associated antifungal properties from roots of different cultivars of *Chysanthemum morifolium* Ramat. Molecules. 25, 2083.

Zhang, B., Li, M., Shi, J., Zeng, M., Zhang, J., Liu, J., Zheng, X., Feng, W., 2023. Six sesquiterpenoids from the stems and leaves of *Chrysanthemum morifolium* Ramat and their anti-asthma activities. *Fitoterapia.* 171, 105633. https://doi.org/10.1016/j.fitote.2023.105633

Zheng, Z.P., Yan, Y., Xia, J., Zhang, S., Wang, M., Chen, J., Xu, Y., 2016. A phenylacetaldehyde-flavonoid adduct, 8-C-(E-phenylethenyl)-norartocarpetin, exhibits intrinsic apoptosis and MAPK pathways-related anticancer potential on HepG2, SMMC-7721 and QGY-7703. *Food Chemistry.* 197, 1085–1092. https://doi.org/10.1016/j.foodchem.2015.11.104

Zhong, H., Zhao, X., Zuo, Z., Sun, J., Yao, Y., Wang, T., Liu, D., Zhao, L., 2016. Combating P-glycoprotein-mediated multidrug resistance with 10-O-phenyl dihydroartemisinin ethers in MCF-7 cells. *European Journal of Medicinal Chemistry.* 108, 720–729. https://doi.org/10.1016/j.ejmech.2015.10.040

Zhu L, Xue L., 2019. Kaempferol suppresses proliferation and induces cell cycle arrest, apoptosis, and DNA damage in breast cancer cells. *Oncology Research.* 27, 629–634. https://doi.org/10.3727/096504018X15228018559434